





Insights into the lower torso in late Miocene hominoid *Oreopithecus bambolii*

Ashley S. Hammond^{a,b,1} , Lorenzo Rook^c , Alisha D. Anaya^a, Elisabetta Cioppi^d, Loïc Costeur^e, Salvador Moyà-Solà^{f,g}, and Sergio Almécija^{a,b,f}

^aDivision of Anthropology, American Museum of Natural History, New York, NY 10024; ^bNew York Consortium of Evolutionary Primatology, New York, NY 10024; ^cPaleo[Fab]Lab, Dipartimento di Scienze della Terra, Università di Firenze, 50121 Florence, Italy; ^dGeologia e Paleontologia, Museo di Storia Naturale, Università di Firenze, 50121 Florence, Italy; ^eDepartment of Geosciences, Naturhistorisches Museum Basel, 4001 Basel, Switzerland; ^fInstitut Català de Paleontologia Miquel Crusafont, Universitat Autònoma de Barcelona, 08193 Barcelona, Spain; and ^gInstitució Catalana de Recerca i Estudis Avançats, 08010 Barcelona, Spain

Edited by Philip Reno, Philadelphia College of Medicine, Philadelphia, PA, and accepted by Editorial Board Member C. O. Lovejoy November 13, 2019 (received for review July 11, 2019)

***Oreopithecus bambolii* (8.3–6.7 million years old) is the latest known hominoid from Europe, dating to approximately the divergence time of the *Pan*-hominin lineages. Despite being the most complete nonhominin hominoid in the fossil record, the *O. bambolii* skeleton IGF 11778 has been, for decades, at the center of intense debate regarding the species' locomotor behavior, phylogenetic position, insular paleoenvironment, and utility as a model for early hominin anatomy. Here we investigate features of the IGF 11778 pelvis and lumbar region based on torso preparations and supplemented by other *O. bambolii* material. We correct several crucial interpretations relating to the IGF 11778 anterior inferior iliac spine and lumbar vertebrae structure and identifications. We find that features of the early hominin *Ardipithecus ramidus* torso that are argued to have permitted both lordosis and pelvic stabilization during upright walking are not present in *O. bambolii*. However, *O. bambolii* also lacks the complete reorganization for torso stiffness seen in extant great apes (i.e., living members of the Hominidae), and is more similar to large hylobatids in certain aspects of torso form. We discuss the major implications of the *O. bambolii* lower torso anatomy and how *O. bambolii* informs scenarios of hominoid evolution.**

ape and human evolution | pelvis | lumbar vertebrae | locomotion

O*reopithecus bambolii* is an insular hominoid species from modern Tuscany and Sardinia, Italy, that is the latest recorded [8.3–6.7 Myr (1)] hominoid from Europe. *O. bambolii* trunk anatomy (2–10) is understood primarily from the taphonomically flattened IGF 11778 skeleton, preliminarily described (11, 12) while embedded in a lignite slab (Fig. 1). Despite the apparently distant relationship between *O. bambolii* and the chimpanzee-human clade (4, 13–16), *O. bambolii* has figured prominently as a model of the chimpanzee-hominin last common ancestor (LCA) (17–20) due to features of the lower torso that have been exclusively aligned with hominins and thus assumed to reflect an adaptation to bipedal locomotion in *O. bambolii* (2, 7, 8, 21, 22). Recently, guided by Miocene hominoids and early hominin *Ardipithecus ramidus* (ARA-VP-6/500), some morphologies seen in early hominins (e.g., lower ilium length, proximal femoral morphology) are understood to be primitive retentions rather than functional traits linked to bipedal adaptation (23–28). Features of the *Ar. ramidus* torso that are argued to have permitted both lordosis and pelvic stabilization during upright walking include a cranio-caudal approximation of the sacroiliac and acetabular joints by a reduction in the lower ilium length, a protuberant anterior inferior iliac spine (AIIS) with a distinct epiphyseal origin, a sagittally oriented and greatly broadened lower iliac isthmus, anterior extension of the lesser gluteals into a position favorable for hip abduction, and likely a relatively mobile lumbar vertebral column (18, 19, 23, 24). It has remained unresolved as to whether these features of *Ar. ramidus* are present in *O. bambolii* (17–19).

Here, we report on features of the pelvic and lumbar regions of *O. bambolii* based on newly prepared elements from IGF 11778 and supplemented by other *O. bambolii* fossils. The revealed pelvic and lumbar anatomy of *O. bambolii* is different from all known taxa and, importantly, differs from past descriptions of the IGF 11778 specimen in key ways.

Results

IGF 11778 Anatomy. Full descriptions of IGF 11778 pelvic and vertebral elements are provided in the *SI Appendix*. The upper vertebral block (*SI Appendix*, Fig. S1) contains the last thoracic (rib-bearing) vertebra and proximal 3 lumbar vertebrae (L1–L3). The well-preserved L1–L3 laminae are proportionally short, unlike the cranio-caudally elongate lumbar laminae (and corresponding elongate vertebral bodies) seen in cercopithecoids and *Ekembo nyanzae* (KNM-MW 13142). A lower vertebral block was preserved in contact with the pelvis (Fig. 1 and *SI Appendix*, Fig. S2). Preparation of the lower vertebral block revealed 2 more lumbar vertebrae, likely the penultimate (L4) and ultimate (L5) lumbar vertebrae, that had been displaced from a more cranial position. The fragmentary lowermost vertebra was identified

Significance

Details of the lower torso anatomy of late Miocene *Oreopithecus bambolii* show that this hominoid differed from both extant great apes (chimpanzees, gorillas, and orangutans) and early hominins (e.g., *Ardipithecus*, *Australopithecus*) in key ways. *O. bambolii* lacked the extreme adaptations for pelvic and lumbar rigidity of extant great apes, but also lacked a hominin-like protruding anterior inferior iliac spine (AIIS), short lower ilium, and abductor mechanism of the hip. The revised understanding of the *O. bambolii* lower torso clarifies the phylogenetic and evolutionary scenarios for this peculiar hominoid.

Author contributions: A.S.H. and S.A. designed research; A.S.H., L.R., A.D.A., S.M.-S., and S.A. performed research; A.S.H. and S.A. analyzed data; and A.S.H., L.R., E.C., L.C., S.M.-S., and S.A. wrote the paper.

The authors declare no competing interest.

This article is a PNAS Direct Submission. P.R. is a guest editor invited by the Editorial Board.

This open access article is distributed under [Creative Commons Attribution-NonCommercial-NoDerivatives License 4.0 \(CC BY-NC-ND\)](https://creativecommons.org/licenses/by-nc-nd/4.0/).

Data deposition: Digital models of original *O. bambolii* specimens used in this study are available on MorphoSource (http://www.morphosource.org/Detail/ProjectDetail/Show/project_id/763), with permission from the curating institutions. The MorphoSource identifier for each model is provided in the *SI Appendix*, Table S1. Comparative data shown herein are available on Figshare (<https://doi.org/10.6084/m9.figshare.11301773.v2>; <https://doi.org/10.6084/m9.figshare.11300978.v1>).

¹To whom correspondence may be addressed. Email: ahammond@amnh.org.

This article contains supporting information online at <https://www.pnas.org/lookup/suppl/doi:10.1073/pnas.1911896116/-DCSupplemental>.

First published December 23, 2019.

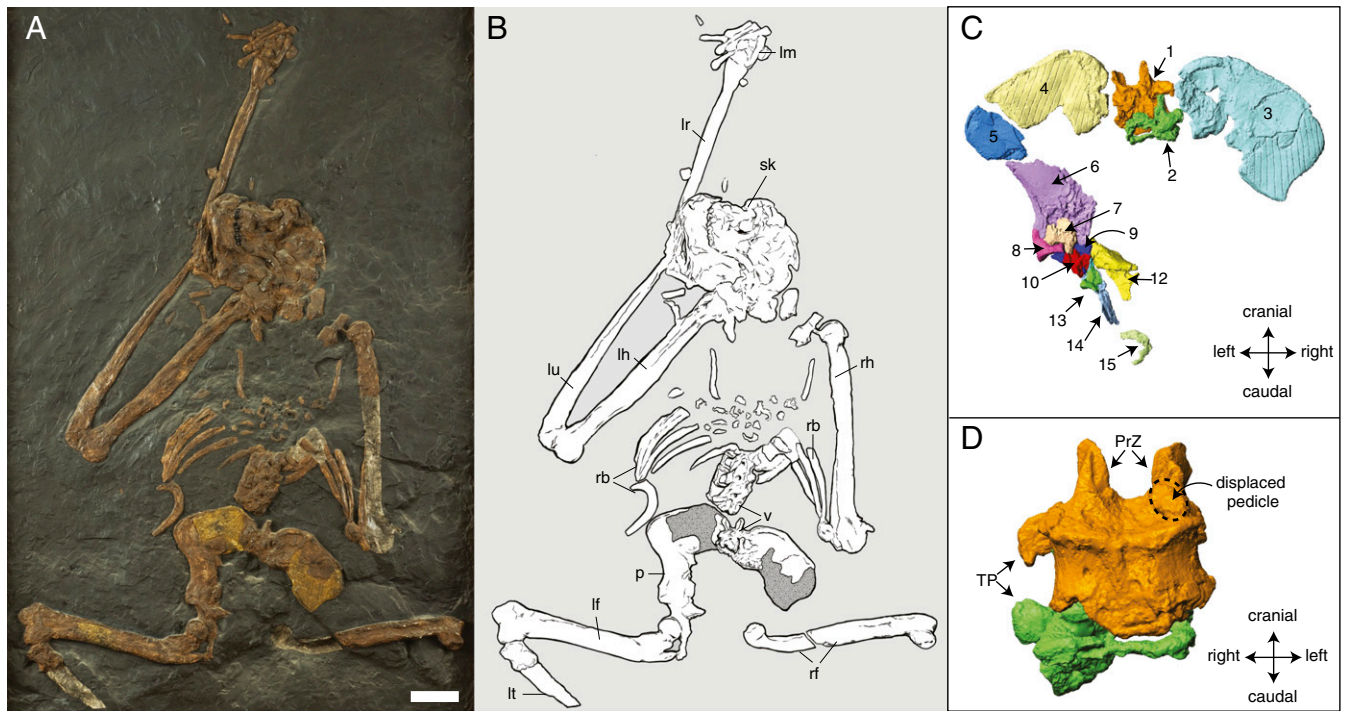


Fig. 1. *O. bambolii*, IGF 11778. (A) Photograph of slab with 5-cm scale. Dashed lines in ilium indicate regions where wax is stabilizing the bone. (B) Composite line drawing. Dark gray indicates regions stabilized by wax. lf, left femur; lh, left humerus; lm, left manus; lt, left tibia; lr, left radius; lu, left ulna; p, pelvis; rb, ribs; rh, right humerus; rf, right femur; sk, skull; v, vertebrae. (C) IGF 11778 pelvis and lower lumbar vertebrae in dorsal view. 1 = penultimate lumbar vertebra; 2 = ultimate lumbar vertebra; 3 = right iliac blade; 4 + 5 = left iliac blade pieces; 6 + 7 = left lower iliac body; 8 = left ilium with cranial portion of acetabular lunate surface; 9 = pubis with small portion of acetabular lunate surface; 10 + 11 = left pubis fragments; 12 = left ischial fragment with a portion of acetabular lunate surface; 14 + 15 = left ischium fragments. (D) Anterior view of ultimate and penultimate vertebrae. PrZ = prezygapophysis; TP = transverse process. Pelvic and vertebral elements are figured in additional high-resolution views in the [SI Appendix](#).

as lumbar based on distinct transverse processes that arise dorsal to the vertebral body, and the cranial orientation of the ultimate transverse process is consistent with being in close proximity to the iliac crest. The IGF 11778 lumbar prezygapophyses, although suffering from some distortion, suggest a medial or oblique joint orientation. Excepting the fragmentary ultimate vertebra, all of the vertebrae have a ventral keel. The sacrum of IGF 11778 is not preserved.

The pelvis itself consists of 13 fragments with significant dorsoventral compression (Fig. 1 and [SI Appendix, Fig. S3](#)). The IGF 11778 ilia are laterally flaring, culminating in a laterally directed anterior superior iliac spine (ASIS), similar to the condition seen in extant great apes and siamangs. The IGF 11778 iliac blades are at the upper limits for relative bi-ASIS breadth in anthropoids (Fig. 2) as preserved, but were most likely closer to the anthropoid average relationship prior to taphonomic flattening. The ilia do not extend as far cranially as in extant great apes, as judged by the distance between the iliac crest and the inferred possible locations of the sacroiliac joint. Although the lower ilium height cannot be exactly measured due to distortion, the range of possible estimates is relatively longer than seen in any hominin (Fig. 2). The sacroiliac joint in IGF 11778 would have been fairly narrow and coronally oriented like that in extant great apes, suggesting that the iliac blades were also coronally oriented (Fig. 2). The coronal orientation of the iliac blades precludes a hip abductor mechanism because the gluteus medius muscle would have been dorsally positioned rather than laterally positioned. The IGF 11778 AIIS (Fig. 3) is not as strongly protruding as previously inferred (2, 6, 7, 17), past inferences being misled by taphonomic crushing and rotation of the lower ilium and AIIS fragments. The pubis of IGF 11778 displays a distinctive tubercle (see [SI Appendix, Fig. S5](#)) which may be homologous to

the adductor longus origin observed in some extant apes (29). The acetabulum is not directly preserved, but the acetabulum diameter can be estimated as about 32 mm based on the preserved femoral head size.

***Oreopithecus bambolii* Lower Torso Morphology.** Other specimens ([SI Appendix, Table S1](#)) further clarify the *O. bambolii* bauplan. Bac 204, which appears to be the transitional vertebra based on pre- and postzygapophyseal orientation, has a demifacet for a rib preserved caudally. The transitional vertebra is thus positioned either cranial to or at the level of the last rib-bearing vertebra, likely permitting more flexion and extension of the lower spine than in most extant great apes (30). Bac 72 (9, 11, 21) preserves the lumbosacral region in articulation with a partial ilium. The Bac 72 ultimate lumbar vertebra displays a cranially inclined transverse process running along the cranial aspect of the iliac crest (Fig. 4), and the tip of the transverse process likely contacted the ilium in vivo. Whereas the ultimate lumbar would have had limited mobility due to proximity to bony structures of the pelvis, the Bac 72 penultimate lumbar was situated above the ilium and less restricted. Bac 182 (2) is an incomplete sacrum that is anteroposteriorly flattened but displays 4 distinct foramina on the left dorsal aspect (Fig. 4), arguing for at least 5 bony segments in the *O. bambolii* sacrum. A total of 5 left foramina yielding 6 segments has been proposed in Bac 182 (2), although we consider one of the foramina to be inconclusive due to state of preservation (see also ref. 31). Bac 182 and Bac 184 preserve fragmentary right iliac blades that show that the sacroiliac joint and iliac blade were paracoronal oriented (Figs. 2 and 4), and that the sacroiliac joint did not have the sharp L shape like cercopithecoids, KNM-MW 13142, and YGSP 41216. The iliac blade tip in Bac 184 does not bear a thickened ASIS. A projecting

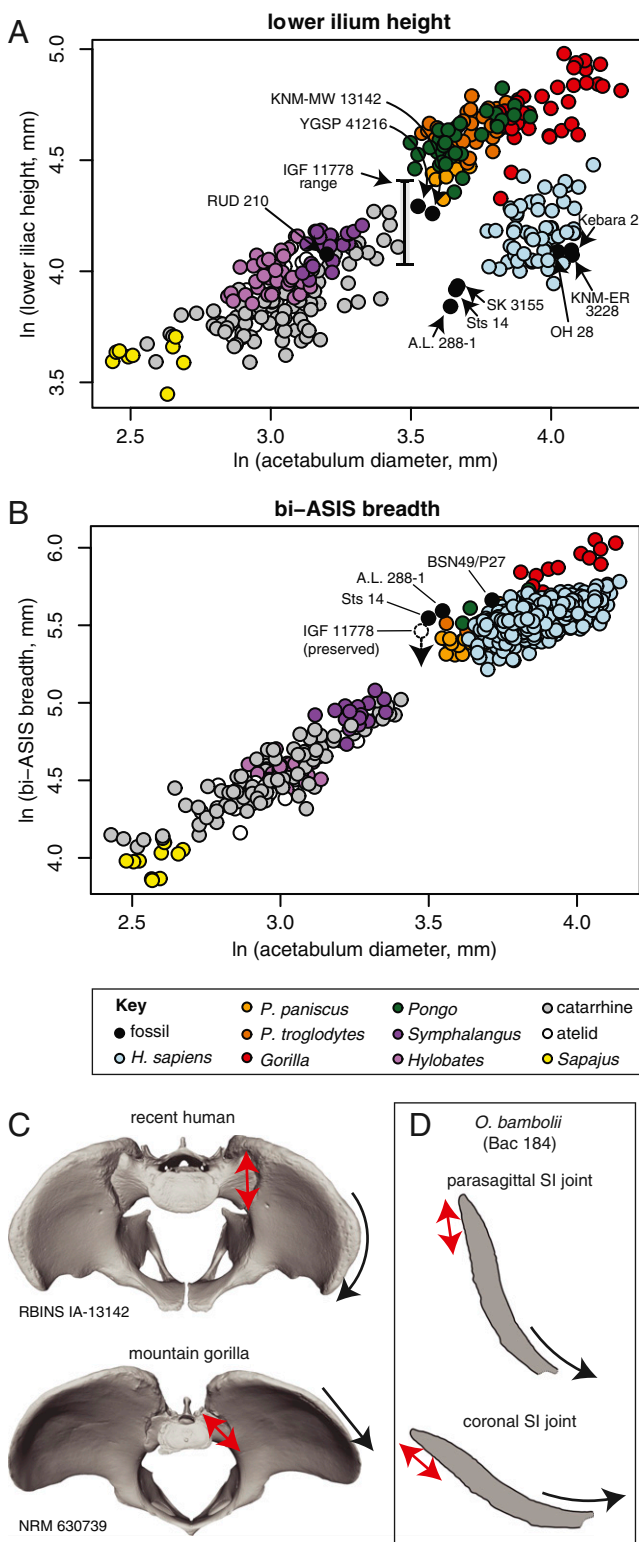


Fig. 2. Pelvic form in anthropoids. (A) Natural log-log scatterplot of lower iliac height and acetabulum diameter in extant ($n = 350$) and fossil anthropoids ($n = 10$). (B) Natural log-log scatterplot of bi-iliac breadth measured across the anterior superior iliac spines and acetabulum diameter in extant ($n = 1,494$) and fossil anthropoids ($n = 4$). IGF 11778 preserved measurement indicated with open circle, with arrow indicating the direction of actual value. (C) Sacroiliac (SI) joint orientation indicated by red arrows; lateral iliac blade orientation indicated by black arrows. (D) The cross-section of Bac 184 (approximating the section location in ref. 41) is consistent with a coronal orientation of the sacroiliac joint and iliac blade, and inconsistent

ischial spine is present in Bac 182 (7) and Bac 71 (11). BA 208 preserves the broken base of the ischial spine and the greater sciatic notch region, which confirms that the lower ilium was not elongated as in extant great apes. Bac 71 preserves the ischial tuberosity which, although small for a primate of this size, is flat and bears a distinct border that is consistent with primate species bearing ischial callosities (Fig. 4). Bac 71 also preserves a pubic symphysis that is incomplete cranially but appears to have been short and mediolaterally broad (11). A second more partial pubic symphysis, BA 208, preserves the cranial-most aspect of the symphysis, a diminutive pubic tubercle adjacent to the symphysis, and the superior aspect of a long pubic ramus. No complete acetabulum is known for *O. bambolii*, but all femoral heads (IGF 11778, IGF 2011V, Bac 74, Bac 75, Bac 76, and Bac 86) have a deeply excavated fovea capitis placed centrally on a highly spherical femoral head, an articular surface distribution that suggests a high level of hip joint mobility (32, 33).

Discussion

IGF 11778 has 5 lumbar vertebrae, as originally interpreted, but element identifications differ from the original descriptions (11). The bone that had been assumed to be a portion of a missing L4 vertebra (11) is actually a displaced portion of pedicle, and so what was thought to be the L5 is likely the L4 (Fig. 1 and *SI Appendix, Fig. S2*). Although IGF 11778 effectively “loses” a lumbar vertebra, it gains one with the discovery of a fragmentary lumbar vertebra distally. Thus, the lower vertebral block in IGF 11778 is composed of 2 displaced lumbar vertebrae that appear to represent the ultimate and penultimate lumbar vertebrae. The postmortem displacement of the lower 2 lumbar vertebrae in IGF 11778 caudally from a more cranial position is further supported by the fairly short iliac blade, which was not long enough to both articulate with the sacrum and entrap a lumbar vertebra caudal to the level of the iliac crest. This interpretation is partially guided by Bac 72, in which the ultimate vertebra’s transverse processes were in contact with the ilium but not situated fully below the cranial aspect of the iliac crest.

The spatial configuration of the IGF 11778 lower torso comes into focus when the upper lumbar block is considered along with the last rib, the lower lumbar block, and the upper ilium (Fig. 4). The distance between the last rib and the cranial rim of the iliac blade spans at least 2 vertebral levels, allowing more flexibility than in extant great apes with ribs that nearly contact the ilium. It is possible that there was a missing vertebra between the upper and lower vertebral blocks in IGF 11778, resulting in an even greater distance between the rib cage and the pelvis. However, given that most of the IGF 11778 lumbar and pelvic regions are preserved, it seems unlikely that an additional midlumbar vertebra was present but no trace of it preserved. A total of 5 non-rib-bearing lumbar vertebrae would be further supported if *O. bambolii* typically had a 6-segment sacrum, as surveys of modern hominoids have never found 6 lumbar vertebrae in combination with a 6-segment sacrum (34–37).

O. bambolii lacked the full suite of adaptations that limit trunk flexion-extension in large-bodied extant great apes. Multiple lines of evidence suggest that the elongate lower ilium seen in extant chimpanzees and orangutans evolved independently (23, 26, 28), so it is unsurprising that *O. bambolii* appears to have a moderate lower ilium length. The presence of 5 lumbar vertebrae in IGF 11778, the modal number of lumbar vertebrae for humans and *Symphalangus* (34), suggests that the lumbar region in *O. bambolii* had more flexion-extension possible than that in extant great apes,

with a parasagittal orientation. The curvature of the Bac 184 gluteal surface would preclude humanlike medial rotation of the anterior iliac blades into the sagittal plane, especially if combined with a narrow sacrum.

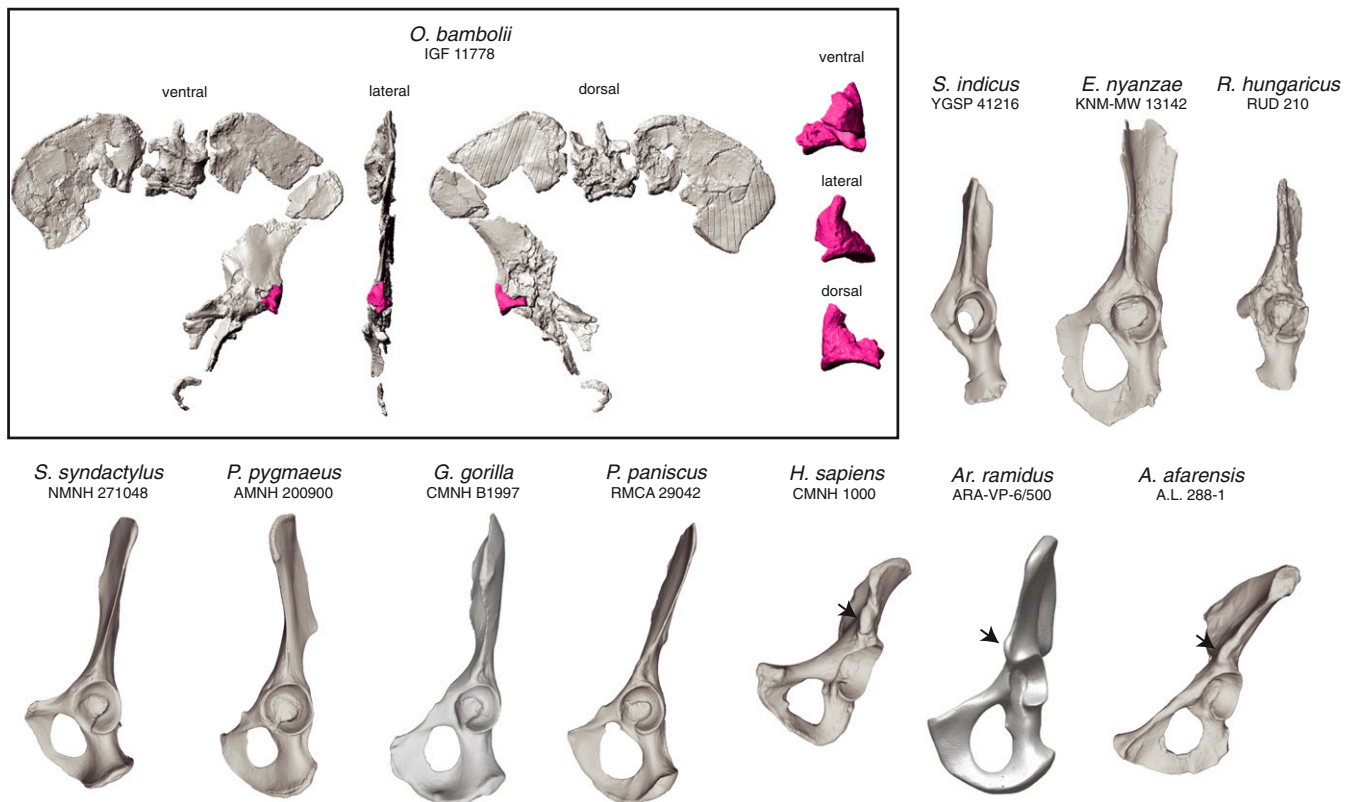


Fig. 3. AIIS comparative anatomy. The IGF 11778 anterior inferior iliac spine (pink) is most comparable to *Gorilla* and *Pan* among extant and fossil hominoids. The hominins (ARA-VP-6/500, A.L. 288-1, and human) all display a projecting sigmoidal AIIS (black arrow) for the rectus femoris muscle and iliofemoral ligament attachment. The *Ardipithecus* (ARA-VP-6/500) figure from ref. 24 was modified with permission from AAAS. Pelves not to scale.

who typically have 3–4 lumbar vertebrae (34–36). The ventral keel on the IGF 11778 L1–L4 vertebral bodies—a trait widely observed in cercopithecoids and hylobatids—suggests that extension of the *O. bambolii* lumbar region was significant enough to necessitate restraint by a well-developed ventral longitudinal ligament (4). The IGF 11778 lumbar prezygapophyses suggest a medial or oblique joint orientation that would restrict rotational movements (38) and favor flexion-extension movements of the spine.

The lower torso in *O. bambolii* is unique among known fossil and living hominoids. The sacroiliac joint (Bac 182, Bac 184) was more coronally oriented, and the iliac blade was substantially more laterally flaring (IGF 11778) than in *Ekembo nyanzae* (39) and *Sivapithecus indicus* (40). Not enough of the *Pierolapithecus catalaunicus* ilium (41) is preserved to compare flaring, but *O. bambolii* exceeds *Rudapithecus hungaricus* (28) in the extent of lateral flare of the ilium (see also Fig. 3). The L4 transverse process origin dorsal to the vertebral body, apparently from the pedicle (see also ref. 14), suggests that the vertebral column was somewhat invaginated (23). The transverse process origin was at least as dorsally positioned as in *P. catalaunicus* (42, 43) and *Morotopithecus bishopi* (44) (*SI Appendix, Fig. S4*), which are intermediate between extant great apes and *E. nyanzae*, *Nacholapithecus kerioi*, and cercopithecoids. The morphology of the *O. bambolii* ischium (Bac 182, IGF 11778) was long and straight like that in other Miocene hominoids (28, 40, 45) and *Ar. ramidus* (24), and was not short and dorsally projecting like that in hylobatids and later hominins (46). The *O. bambolii* ischial spine (Bac 182, Bac 71) is comparable to that of modern humans in absolute size, but ischial spines are known in hominins, hylobatids, and some fossil lemurs (47). One of the most intriguing interpretations raised here is the possibility of ischial callosities in *O.*

bambolii (Fig. 4; Bac 71 and IGF 11778), a feature found only in hylobatids among extant hominoids.

Locomotor adaptation in *O. bambolii* has been controversial for more than half a century, with the most controversial claims being that *O. bambolii* either was a bipedal ape (7, 8, 10, 22, 48) or used inverted suspension (47). Although the long forelimb of *O. bambolii* suggests that forelimb-dominated climbing behaviors were a key part of the locomotor repertoire (2, 4, 6, 11, 49, 50), the plesiomorphic hand length proportions have a relatively balanced thumb-to-digits ratio (51, 52) that does not favor inverted suspensory behaviors per se. Regarding the bipedal hypothesis, the *O. bambolii* lower torso has figured prominently in the most recent arguments, with a focus on the relatively short pelvis (2, 6, 7, but note Fig. 2), a projecting AIIS region (2, 6, 7, 10, but see Fig. 3), a short pubic symphysis (7), a long and straight pubis (7), large ischial spines (7, but see ref. 47), trabecular networks of the ilium (8), and human-like wedging and interfacet positioning of the lumbar vertebrae (7, but see ref. 9). The argument made in those studies was that *O. bambolii* engaged in a bizarre type of bipedal locomotion different from that of hominins. The argument made in previous studies was in close relationship to the paleoecological context: *O. bambolii* evolved from an unidentified ancestor in an endemic paleo-island during the late Miocene, with limited trophic resources and a lack of terrestrial predators characteristic of such environments. Following this hypothesis, *O. bambolii* would have developed an array of adaptations, including features of the hands and feet (see refs. 7, 8, 10, 22, 48, and 51), that allowed more efficient bipedal posture and locomotion than that reported in living apes [e.g., orangutans regularly rely on hand-assisted bipedality (53)].

Inferences about bipedal adaptation (or lack thereof) in *O. bambolii* are limited to a model that has been shaped by our

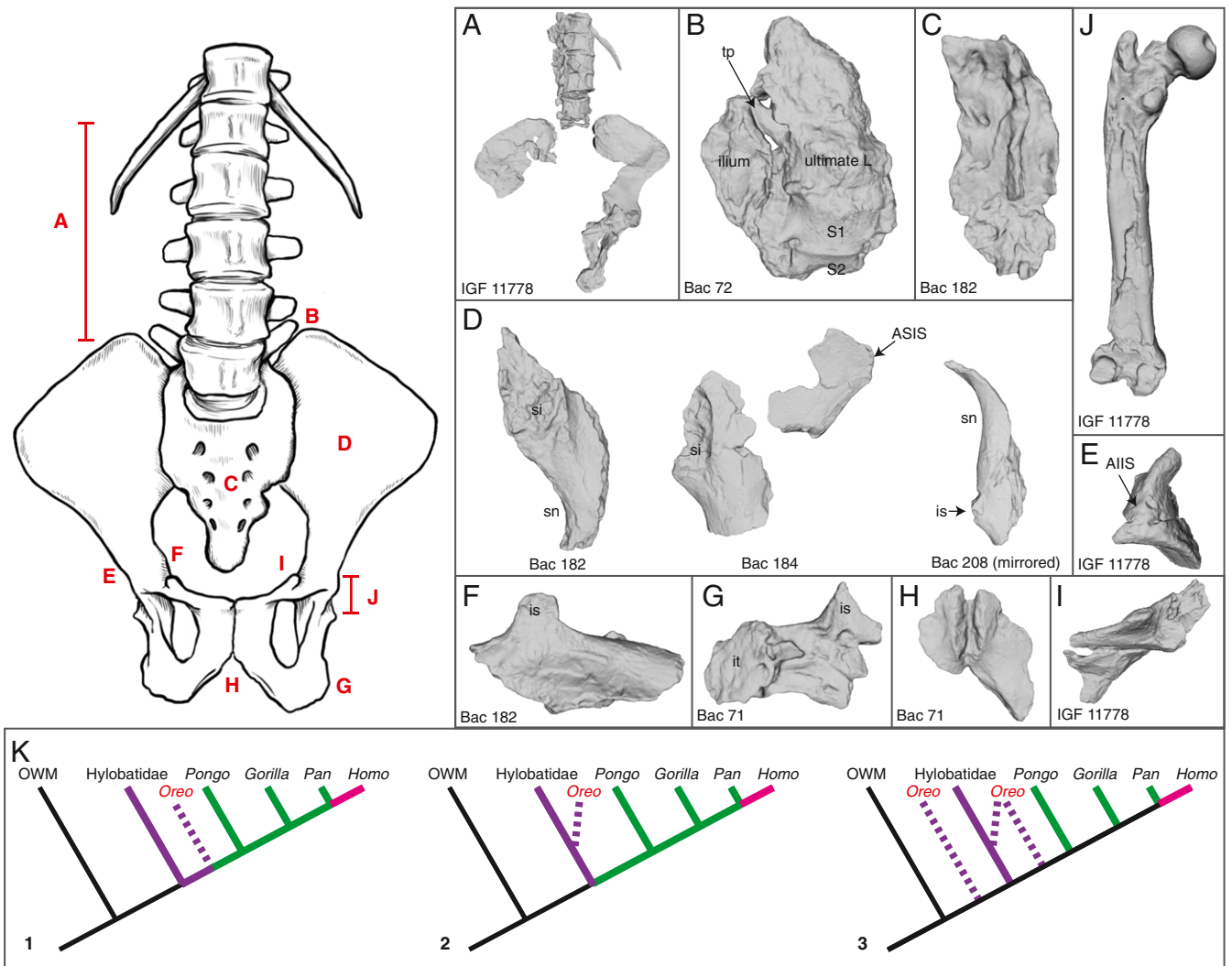


Fig. 4. The *O. bambolii* lower torso and evolutionary scenarios. (A) The lumbar spine was moderately flexible with 5 vertebrae, with at least 2 vertebral levels separating the last rib and the upper pelvis. (B) The transverse process (tp) of the last lumbar vertebra ran cranially along the iliac crest and was entrapped by the ilium. (C) The sacrum had 5 or 6 segments. (D) The sacroiliac joint (si) was narrow and paracoronal oriented, and the ilium was not dorsally retroflexed as evidenced by the shallow greater sciatic notch (sn). The lower ilium was moderate in length. The ASIS was not thick. (E) The AIIS was not protruding. (F) The ischium had a strongly projecting ischial spine (is). (G) The ischial tuberosity (it) may have been callosity-bearing. (H) The pubic symphysis was likely craniocaudally abbreviated. (I) The pubis was long, with a prominent adductor longus origin site. (J) The hip joint was not adapted for large cranially directed loads, as evidenced by the femoral head. (K) 3 evolutionary scenarios are compatible with these morphologies (refer to text for descriptions of the 3 scenarios). Evolutionary regimes are indicated by colors along the tree branches: purple, hylobatid-like (specifically *Symphalangus*-like); green, great ape; pink, hominin. Location of *O. bambolii* ("Oreo" label) indicated in each scenario by dashed line(s).

understanding of bipedality in hominins specifically. The wide human sacrum positions the iliac blade more laterally relative to the midsagittal plane and allows medial rotation of the anterior blade without impinging on the abdominal cavity (54, 55). The narrow sacrum (Bac 182, Bac 72) and paracoronal oriented sacroiliac joint (Bac 182, Bac 184) in *O. bambolii* would preclude human-like medial rotation of the anterior iliac blades into the sagittal plane (Fig. 2). The paracoronal orientation of the ilium effectively eliminates the possibility of a hominin-like gluteal abductor mechanism, which is necessary for efficient single-limb support. Whereas hominins have a muscular configuration that favors abduction at the hip to maintain mediolateral trunk stability during bipedal gait, the hindlimb of *O. bambolii* may have been configured to provide powerful thigh adduction during climbing based on the protuberant adductor longus muscle origin (SI Appendix, Fig. S5). Moreover, the *O. bambolii* upper ilia were not retroflexed like those of hominins, as evidenced by the

shallow greater sciatic notch (Bac 182, BA 208). The *O. bambolii* femoral heads (IGF 11778, IGF 2011V, Bac 74, Bac 75, Bac 76, Bac 86) show a deeply excavated fovea capitis that greatly reduced the bone volume of the femoral head. The femoral heads and sacroiliac joint (Bac 182, Bac 184) were not adapted for the transmission of large, vertically directed loads like hominins (Fig. 4), especially genus *Homo*. The ischium in *O. bambolii* (Bac 182, IGF 11778) was fairly long and straight, which would be advantageous for vertical climbing but reduced bipedal walking economy (56). As noted elsewhere, the *O. bambolii* femur (IGF 11778) was relatively short compared not just to hominins but to extant hominoids and cercopithecoids as well (49). Although certainly more capable of bipedal positional behaviors than extant great apes, *O. bambolii* lacked features of the lower torso related to biomechanically efficient habitual and/or obligate bipedalism in hominins.

Finally, how does a revised understanding of *Oreopithecus* inform evolutionary scenarios? *Oreopithecus* was an insular, swamp-dwelling hominoid subjected to a very different array of selective pressures than African apes and hominins, yet it provides insight into a hominoid bauplan that was not derived in the manner of extant apes and humans. The *Oreopithecus* lower torso shows moderate reorganization compared to early and middle Miocene hominoids, but it does not display a fully rigid lumbar region and elongate ilium like those of the extant great apes. Compared to extant taxa, *Oreopithecus* shares a number of affinities with *Symphalangus*, including 5 lumbar vertebrae, transverse processes that arose on the pedicle, an ilium that was not elongated but fairly broad, an ischial spine, and (possibly) ischial callosities. There are at least 3 evolutionary scenarios compatible with these features of the lower torso.

The first evolutionary scenario is that *Oreopithecus* and *Symphalangus* share similarities because they both retain plesiomorphic characters of crown Hominoidea (which are synapomorphic relative to stem hominoids). This scenario implies that some of the torso features associated with orthogrady evolved at the origins of the hominoid crown group at ~17 Myr (57). In this scenario, *Oreopithecus* could be a stem member of the Hominidae (Fig. 4). The monkey-like torso anatomy inferred for *Ekembo* (39, 45) and *Sivapithecus* (40) would require that these taxa be outside the hominoid crown group, secondarily reverted, or that they retain the plesiomorphic condition.

The second evolutionary scenario is that *Oreopithecus* was a member of the Hylobatidae (see also ref. 58). This scenario would expand the geographical and body size ranges that are known for (extant) hylobatids. However, given that the modern hylobatid diversification began around 6.7 Myr (57), *Oreopithecus* would necessarily be a stem hylobatid (Fig. 4). Moreover, this scenario implies that the long and curved phalanges associated with brachiation and the reduction in body size dimorphism seen in modern hylobatids evolved later within this group. Certainly, with males larger than 30 kg (49), it would have been impossible for *O. bambolii* to have crossed arboreal gaps via leaps or ricochet brachiation like extant hylobatids.

The third evolutionary scenario is that *Oreopithecus* torso morphologies can be explained by convergent evolution. There is a trend within fossil hominoids for increased reliance on orthograde behaviors through time (59), and selection for orthogrady—possibly in multiple hominoid lineages and at body sizes not sampled by extant hominoid taxa—could explain the described torso features. Some features, such as ischial callosities, would represent plesiomorphic retentions of the *Oreopithecus* lineage. In this scenario, *Oreopithecus* could be aligned with any hominoid group (e.g., stem hominoids, hylobatids, hominids; Fig. 4). Again, the monkey-like torso anatomies inferred for earlier fossil apes could be present for the same reasons posed in the first evolutionary scenario.

Future work incorporating other regions of the skeleton might clarify which of these scenarios is the most credible. All of these

scenarios reaffirm late Miocene *O. bambolii* as an important morphological and behavioral point of comparison with models of hominin origins.

Materials and Methods

O. bambolii fossils were measured with Mitutoyo digital calipers. IGF 11778 and 2011V were studied at the Museo di Storia Naturale at the University of Florence, and all other *O. bambolii* specimens were studied at the Naturhistorisches Museum Basel. The IGF 11778 pelvis was prepared from 1994 to 2000 with permission of Professor Danilo Torre at the Institut Català Paleontologia Miquel Crusafont.

The IGF 11778 minimum lower ilium height estimate (58.4 mm) is the distance from the acetabulum to the preserved edge of the lower ilium fragment (fragment 6 in Fig. 1) plus 1/2 the femoral head diameter to account for flattening of the acetabulum. The IGF 11778 maximum lower ilium height estimate (80.0 mm) is the distance from the acetabulum border to the most cranial position where the sacroiliac joint could reasonably have been positioned, based on the other elements and the original position in the lignite slab.

Anthropoid comparative data for lower iliac height (26) and bi-iliac breadth (60, 61) were gathered from published sources. Fossil bi-ASIS data were gathered from ref. 62. Acetabulum dimensions were measured directly or gathered from refs. 63 and 64, and the IGF 11778 acetabulum size was estimated following regressions described in the *SI Appendix, Table S2*. Comparative extant specimens shown in figures are from the American Museum of Natural History (AMNH), the Cleveland Museum of Natural History (CMNH), the Smithsonian Institution (NMNH), the Royal Museum for Central Africa (RMCA), the Royal Belgian Institute of Natural Sciences (RBINS), and the Swedish Museum of Natural History (NRM). Fossils were compared at the Ethiopian Authority for Research and Conservation of the Cultural Heritage, the Peabody Museum at Harvard, the Institut Català de Paleontologia Miquel Crusafont, the National Museums of Kenya, and via personal casts.

High-resolution 3D surface data of the *O. bambolii* fossils were generated using a Geomagic Capture scanner (3D Systems, Rock Hill, SC) or an EinScan Pro+ 3D surface scanner (SHINING 3D Tech Co., Hangzhou, China). Surface data were prepared in Geomagic Studio following published postprocessing protocols (65).

Data Availability. Digital models of original *O. bambolii* specimens used in this study are available for download on MorphoSource (<https://www.morphosource.org>; project number P763) with permission from the curating institutions. The MorphoSource identifier for each model is provided (*SI Appendix, Table S1*). Anthropoid linear data that were used in this study have been published as datasets in the Figshare online repository (66, 67).

ACKNOWLEDGMENTS. We thank D. Begun, B. Demes, S. Maddux, E. Middleton, M. Muchlinski, I. Pellejero, D. Pilbeam, J. M. Plavcan, D. Torre, C. V. Ward, and K. Younkun for assistance, data, comparative casts, and/or helpful critique. T. D. White and the Ethiopian Authority for Research and Conservation of the Cultural Heritage are thanked for facilitating study of ARA-VP-6/500. All curators and staff at curating institutions are thanked for facilitating access to comparative material. Funding was provided by the Wenner-Gren Foundation, the Leakey Foundation, the Centres de Recerca de Catalunya Programme and 2017 86 Grup de Recerca Consolidat (Generalitat de Catalunya), and Spanish project CGL2017-82654-P (Fondo Europeo de Desarrollo Regional).

1. L. Rook, O. Oms, M. G. Benvenuti, M. Papini, Magnetostratigraphy of the Late Miocene Baccinello–Cinigiano basin (Tuscany, Italy) and the age of *Oreopithecus bambolii* faunal assemblages. *Palaeogeogr. Palaeoclimatol. Palaeoecol.* **305**, 286–294 (2011).
2. W. L. Straus, *The Classification of Oreopithecus. Classification and Human Evolution*, S. L. Washburn, Ed. (Aldine, Chicago, 1963), pp. 146–177.
3. J. Biegert, R. Maurer, Rumpfskelettlänge, Allometrien und Körperproportionen bei catarrhinen Primaten. [in German]. *Folia Primatol. (Basel)* **17**, 142–156 (1972).
4. E. E. Sarmiento, The phylogenetic position of *Oreopithecus* and its significance in the origin of the Hominoidea. *Am. Mus. Novit.* **2881**, 1–44 (1987).
5. J. Stern, W. Jungers, Body size and proportions of the locomotor skeleton in *Oreopithecus bambolii*. *Am. J. Phys. Anthropol.* **66**, 233 (1985).
6. T. Harrison, “The implications of *Oreopithecus bambolii* for the origins of bipedalism” in *Origine(s) de la bipédie chez les hominidés*, Y. Coppens, B. Senut, Eds. (Editions du Centre National de la Recherche Scientifique, Paris, 1991), pp. 235–244.
7. M. Köhler, S. Moyà-Solà, Ape-like or hominid-like? The positional behavior of *Oreopithecus bambolii* reconsidered. *Proc. Natl. Acad. Sci. U.S.A.* **94**, 11747–11750 (1997).
8. L. Rook, L. Bondioli, M. Köhler, S. Moyà-Solà, R. Macchiarelli, *Oreopithecus* was a bipedal ape after all: Evidence from the iliac cancellous architecture. *Proc. Natl. Acad. Sci. U.S.A.* **96**, 8795–8799 (1999).
9. G. A. Russo, L. J. Shapiro, Reevaluation of the lumbosacral region of *Oreopithecus bambolii*. *J. Hum. Evol.* **65**, 253–265 (2013).
10. W. L. Straus Jr, Fossil evidence of the evolution of the erect, bipedal posture. *Clin. Orthop.* **25**, 9–19 (1962).
11. A. H. Schultz, Einige Beobachtungen und Masse am Skelett von *Oreopithecus*: Im Vergleich mit anderen catarrhinen Primaten. *Z. Morphol. Anthropol.* **50**, 136–149 (1960).
12. W. L. Straus, A new *Oreopithecus* skeleton. *Science* **128**, 523 (1958).
13. T. Harrison, A reassessment of the phylogenetic relationships of *Oreopithecus bambolii* gervais. *J. Hum. Evol.* **15**, 541–583 (1986).
14. T. Harrison, L. Rook, “Enigmatic anthropoid or misunderstood ape? The phylogenetic status of *Oreopithecus bambolii* reconsidered” in *Function, Phylogeny, and Fossils: Miocene Hominoid Evolution and Adaptations*, D. R. Begun, C. V. Ward, M. D. Rose, Eds. (Plenum Press, New York, 1997), pp. 327–362.

15. E. Delson, An anthropoid enigma: Historical introduction to the study of *Oreopithecus bambolii*. *J. Hum. Evol.* **15**, 523–531 (1986).
16. S. Moyà-Solà, M. Köhler, The phylogenetic relationships of *Oreopithecus bambolii* Gervais, 1872. *C R Acad Sci Paris* **324**, 141–148 (1997).
17. E. E. Sarmiento, Comment on the paleobiology and classification of *Ardipithecus ramidus*. *Science* **328**, 1105, author reply 1105 (2010).
18. T. D. White, G. Suwa, C. O. Lovejoy, Response to comment on the paleobiology and classification of *Ardipithecus ramidus*. *Science* **328**, 1105 (2010).
19. T. D. White, C. O. Lovejoy, B. Asfaw, J. P. Carlson, G. Suwa, Neither chimpanzee nor human, *Ardipithecus* reveals the surprising ancestry of both. *Proc. Natl. Acad. Sci. U.S.A.* **112**, 4877–4884 (2015).
20. B. Wood, T. Harrison, The evolutionary context of the first hominins. *Nature* **470**, 347–352 (2011).
21. J. Hürzeler, *Oreopithecus bambolii* Gervais, a preliminary report, *Verh. naturf. Ges. Basel* **69**, 1–47 (1958).
22. W. L. Straus, *Oreopithecus bambolii*. *Science* **126**, 345–346 (1957).
23. C. O. Lovejoy, G. Suwa, S. W. Simpson, J. H. Matternes, T. D. White, The great divides: *Ardipithecus ramidus* reveals the postcrania of our last common ancestors with African apes. *Science* **326**, 100–106 (2009).
24. C. O. Lovejoy, G. Suwa, L. Spurlock, B. Asfaw, T. D. White, The pelvis and femur of *Ardipithecus ramidus*: The emergence of upright walking. *Science* **326**, 71–71e6 (2009).
25. T. D. White et al., *Ardipithecus ramidus* and the paleobiology of early hominids. *Science* **326**, 75–86 (2009).
26. A. S. Hammond, S. Almécija, Lower ilium evolution in apes and hominins. *Anat. Rec. (Hoboken)* **300**, 828–844 (2017).
27. S. Almécija et al., The femur of *Orrorin tugenensis* exhibits morphometric affinities with both Miocene apes and later hominins. *Nat. Commun.* **4**, 2888 (2013).
28. C. V. Ward, A. S. Hammond, J. M. Plavcan, D. R. Begun, A late Miocene hominoid partial pelvis from Hungary. *J. Hum. Evol.* **136**, 102645 (2019).
29. B. M. Shearer, M. Muchlinski, A. S. Hammond, Large pelvic tubercle in orangutans relates to the adductor longus muscle. *PeerJ* **7**, e7273 (2019).
30. S. A. Williams, Placement of the diaphragmatic vertebra in catarrhines: Implications for the evolution of dorsostability in hominoids and bipedalism in hominins. *Am. J. Phys. Anthropol.* **148**, 111–122 (2012).
31. M. Haessler, S. A. Martelli, T. Boeni, Vertebral numbers of the early hominid lumbar spine. *J. Hum. Evol.* **43**, 621–643 (2002).
32. L. M. MacLatchy, W. H. Bossert, An analysis of the articular surface distribution of the femoral head and acetabulum in anthropoids, with implications for hip function in Miocene hominoids. *J. Hum. Evol.* **31**, 425–453 (1996).
33. A. S. Hammond, In vivo baseline measurements of hip joint range of motion in suspensory and nonsuspensory anthropoids. *Am. J. Phys. Anthropol.* **153**, 417–434 (2014).
34. S. A. Williams, E. R. Middleton, C. I. Villamil, M. R. Shattuck, Vertebral numbers and human evolution. *Am. J. Phys. Anthropol.* **159** (suppl. 61), S19–S36 (2016).
35. M. A. McCollum, B. A. Rosenman, G. Suwa, R. S. Meindl, C. O. Lovejoy, The vertebral formula of the last common ancestor of African apes and humans. *J. Exp. Zool. B Mol. Dev. Evol.* **314**, 123–134 (2010).
36. D. Pilbeam, The anthropoid postcranial axial skeleton: Comments on development, variation, and evolution. *J. Exp. Zool. B Mol. Dev. Evol.* **302**, 241–267 (2004).
37. S. A. Williams, Variation in anthropoid vertebral formulae: Implications for homology and homoplasy in hominoid evolution. *J. Exp. Zool. B Mol. Dev. Evol.* **318**, 134–147 (2012).
38. L. J. Shapiro, “Functional morphology of the vertebral column in primates” in *Postcranial Adaptation in Non-Human Primates*, D. Gebo, Ed. (Northern Illinois University Press, DeKalb, 1993).
39. C. V. Ward, Torso morphology and locomotion in *Proconsul nyanzae*. *Am. J. Phys. Anthropol.* **92**, 291–328 (1993).
40. M. E. Morgan et al., A partial hominoid innominate from the Miocene of Pakistan: Description and preliminary analyses. *Proc. Natl. Acad. Sci. U.S.A.* **112**, 82–87 (2015).
41. A. S. Hammond, D. M. Alba, S. Almécija, S. Moyà-Solà, Middle Miocene *Pierolapithecus* provides a first glimpse into early hominid pelvic morphology. *J. Hum. Evol.* **64**, 658–666 (2013).
42. S. Moyà-Solà, M. Köhler, D. M. Alba, I. Casanovas-Vilar, J. Galindo, *Pierolapithecus catalaunicus*, a new Middle Miocene great ape from Spain. *Science* **306**, 1339–1344 (2004).
43. I. Susanna, D. M. Alba, S. Almécija, S. Moyà-Solà, The vertebral remains of the late Miocene great ape *Hispanopithecus laietanus* from Can Llobateres 2 (Vallès-Penedès Basin, NE Iberian Peninsula). *J. Hum. Evol.* **73**, 15–34 (2014).
44. L. MacLatchy, D. Gebo, R. Kityo, D. Pilbeam, Postcranial functional morphology of *Morotopithecus bishopi*, with implications for the evolution of modern ape locomotion. *J. Hum. Evol.* **39**, 159–183 (2000).
45. C. V. Ward, A. Walker, M. F. Teaford, I. Odhiambo, Partial skeleton of *Proconsul nyanzae* from Mfangano Island, Kenya. *Am. J. Phys. Anthropol.* **90**, 77–111 (1993).
46. K. L. Lewton, J. E. Scott, Ischial form as an indicator of bipedal kinematics in early hominins: A test using extant anthropoids. *Anat. Rec. (Hoboken)* **300**, 845–858 (2017).
47. R. E. Wunderlich, A. Walker, W. L. Jungers, Rethinking the positional repertoire of *Oreopithecus*. *Am. J. Phys. Anthropol.* **528**, 282 (1999).
48. B. Kummer, Die Biomechanik der aufrechten Haltung. *Mitt. Naturforsch. Ges.* **22**, 239–259 (1965).
49. W. L. Jungers, Body size and morphometric affinities of the appendicular skeleton in *Oreopithecus bambolii* (IGF 11778). *J. Hum. Evol.* **16**, 445–456 (1987).
50. M. D. Rose, “Functional and phylogenetic features of the forelimb in Miocene hominoids” in *Function, Phylogeny and Fossils: Miocene Hominoid Evolution and Adaptation*, D. R. Begun, C. V. Ward, M. D. Rose, Eds. (Plenum Press, New York, 1997), pp. 79–100.
51. S. Moyà-Solà, M. Köhler, L. Rook, Evidence of hominid-like precision grip capability in the hand of the Miocene ape *Oreopithecus*. *Proc. Natl. Acad. Sci. U.S.A.* **96**, 313–317 (1999).
52. S. Almécija, M. Shrewsbury, L. Rook, S. Moyà-Solà, The morphology of *Oreopithecus bambolii* pollical distal phalanx. *Am. J. Phys. Anthropol.* **153**, 582–597 (2014).
53. S. K. Thorpe, R. L. Holder, R. H. Crompton, Origin of human bipedalism as an adaptation for locomotion on flexible branches. *Science* **316**, 1328–1331 (2007).
54. C. O. Lovejoy, Evolution of human walking. *Sci. Am.* **259**, 118–125 (1988).
55. C. O. Lovejoy, The natural history of human gait and posture. Part 1. Spine and pelvis. *Gait Posture* **21**, 95–112 (2005).
56. E. E. Kozma et al., Hip extensor mechanics and the evolution of walking and climbing capabilities in humans, apes, and fossil hominins. *Proc. Natl. Acad. Sci. U.S.A.* **115**, 4134–4139 (2018).
57. M. S. Springer et al., Macroevolutionary dynamics and historical biogeography of primate diversification inferred from a species supermatrix. *PLoS One* **7**, e49521 (2012).
58. L. Rüttemeyer, *Über Pliocen und Eisperiode auf beiden Seiten der Alpen* (Georg, Basel, 1876).
59. M. Nakatsukasa, Y. Kunimatsu, *Nacholapithecus* and its importance for understanding hominoid evolution. *Evol. Anthropol.* **18**, 113–119 (2009).
60. C. V. Ward, S. D. Maddux, E. R. Middleton, Three-dimensional anatomy of the anthropoid bony pelvis. *Am. J. Phys. Anthropol.* **166**, 3–25 (2018).
61. B. M. Auerbach, C. B. Ruff, Human body mass estimation: A comparison of “morphometric” and “mechanical” methods. *Am. J. Phys. Anthropol.* **125**, 331–342 (2004).
62. J. M. Kibii et al., A partial pelvis of *Australopithecus sediba*. *Science* **333**, 1407–1411 (2011).
63. S. W. Simpson et al., A female *Homo erectus* pelvis from Gona, Ethiopia. *Science* **322**, 1089–1092 (2008).
64. J. M. Plavcan, A. S. Hammond, C. V. Ward, Calculating hominin and nonhuman anthropoid femoral head diameter from acetabular size. *Am. J. Phys. Anthropol.* **155**, 469–475 (2014).
65. A. S. Hammond, J. M. Plavcan, C. V. Ward, A validated method for modeling anthropoid hip abduction in silico. *Am. J. Phys. Anthropol.* **160**, 529–548 (2016).
66. A. S. Hammond, C. V. Ward, Data from “Bi-iliac breadth for anthropoids.” Figshare. <https://doi.org/10.6084/m9.figshare.11301773.v2>. Deposited 2 December 2019.
67. A. S. Hammond, S. Almécija, Data from “Lower ilium length in anthropoids.” Figshare. <https://doi.org/10.6084/m9.figshare.11300978.v1>. Deposited 30 November 2019.